Experimental verification of a substructure-based model to describe pedestrian-bridge interaction

Daniel Gomez, S.M.ASCE[1,2], Shirley J. Dyke[3], and Shirley Rietdyk[4]

[1]Research Assistant, Lyles School of Civil Engineering, Purdue University, West Lafayette, USA.
E-mail: dgomezp@purdue.edu

[2]Associate Professor, School of Civil Engineering, Universidad del Valle, Cali, Colombia.

[3]Professor, School of Civil and Mechanical Engineering, Purdue University, West Lafayette, USA.

[4]Professor, Department of Health and Kinesiology, Purdue University, West Lafayette, USA.

ABSTRACT

An increasing number of structures, and in particular pedestrian bridges, are experiencing excessive vibration levels when they are dynamically excited by humans in motion. Although several models have been presented to incorporate the influence of a single pedestrian traversing a flexible structure, there is no commonly accepted method to include the presence of dynamic interactions that results in complex time-varying and coupled dynamics. Here a new coupled model is presented and shown to be effective in modeling the coupled dynamics associated with pedestrian-bridge interaction (PBI). Through a series of experiments involving three human subjects walking under different conditions, the model is validated in accordance to their capability to reproduce and replicate the complex vibration patterns observed on a full-scale bridge with a single pedestrian. The results demonstrate that the PBI model provides an effective and reliable approach to simulate human-structure interaction.

INTRODUCTION

In recent years, footbridges have become an important component of our urban infrastructure. These structures serve to provide safe means for pedestrians to pass over urban roads and highways, but have also been included as integral elements in the effort to revitalize and create more pedestrian-friendly communities. However, an increasing number of pedestrian bridges have reported problems with excessive vibrations induced by human traffic, although most of them are designed according to existing standards and guidelines. Excessive vibration may be attributed to high structural flexibility, low bridge weight, or longer spans between supports (Ellingwood and Tallin 1984; Sachse et al. 2003). Thus, certain footbridges are more sensitive to human-induced dynamic loading than others. Consequently, these bridges exhibit excessive vibrations yielding, in some cases, damage and fatigue (Kim et al. 2008). Furthermore, conditions of serviceability often control the design of this type of structure (Sánchez et al. 2013). Unfortunately, most design-and-construction codes neglect pedestrian-bridge interactions, and simply assume that the pedestrian can be represented as a moving load traversing the bridge (Blanchard et al. 1977; Rainer et al. 1988). However, this approach ignores the dynamic effects of human-structure interaction (HSI) which is viewed as the fundamental source of uncertainty in the dynamic response of footbridges.

At this time serviceability guidelines are limited in considering the fact that changes occur in the dynamic properties of pedestrian bridges due to these dynamic interactions with moving pedestrians. Serviceability guidelines do not accurately predict their dynamic responses, and thus existing standards suffer from inconsistent and sometimes illogical design solutions, demonstrating significant gaps in knowledge remain (Roos 2009; Zuo et al. 2012; Van Nimmen et al. 2014). Even with recent advances in load models and response predictions, measured responses from pedestrian bridges in operation often deviate greatly from those predicted (Živanović et al. 2009). The main reason for this gap is that experimental studies of HSI, as well as the analytical models available to describe the loads produced by human walking, are unable to adequately reproduce the dynamic interaction between the two systems (Shahabpoor et al. 2013). As a consequence, our ability to design for these loads is still limited. Because the vibration requirements due to human loads are a dominant factor in the actual structural response of pedestrian bridges, better modeling approaches are critically needed.

Several analytical models have been developed in the last three decades to predict footbridge responses due to human walking in the lateral and vertical direction. Many attempts to model human-induced effects in the lateral direction took place soon after the Millennium bridge exhibited unexpected large amplitude vibrations on its opening day in 2000 (Dallard et al. 2001; Roberts 2003; Ricciardelli and Pizzimenti 2007; Eckhardt et al. 2007; Venuti et al. 2007; Macdonald 2009). Also, of the several analytical models of human-induced vertical vibration that have been proposed, most of them consider a single pedestrian as a deterministic moving harmonic force (Živanović et al. 2005), neglecting the interaction as a bi-directional effect between the pedestrian and the oscillating bridge. Generally speaking, this approach is called the moving force problem. In this strategy, the vertical ground reaction force (GRF) generated by a pedestrian on a "rigid" floor is applied as a moving load. In fact, this straightforward approach is often adopted by the most common international standards and building codes (Archbold et al. 2011; Živanović et al. 2010).

Improving upon this approach, different mathematical models have been proposed to describe pedestrian-bridge interaction. Using a spring-mass-damper system to represent a person crossing the bridge is one approach derived from the moving oscillator problem (Fanning et al. 2005; Toso et al. 2013; Pfeil et al. 2014; Gomez et al. 2015b), and a periodic force, which describes the GRF, is applied to the footbridge at the pedestrian location (Archbold et al. 2011; Jimenez-Alonso et al. 2016). Early developments in biomechanics and robotics representing the human locomotion as an inverted pendulum were explained by Mochon and McMahon (1980), Onyshko and Winter (1980), Alexander (1995), and Whittington and Thelen (2009). However, these bipedal models were initially created to describe a human while walking on a rigid surface. Recently, more detailed models have been motivated by these bipedal representations and were adapted for a moving surface (Bocian et al. 2013; Qin et al. 2013a; Qin et al. 2013b). Nevertheless, despite the fact that the equations for the bipedal alone are quite simple, when the structure is included, the system equations become more complex, and accounting for the change of location of the pedestrian yields a time-varying system.

In this paper we propose a pedestrian-bridge interaction (PBI) model to predict the vertical dynamic response of a footbridge traversed by a single pedestrian. A modular approach is used to represent the pedestrian-bridge system as coupled subsystems that interact dynamically with each other. Thus, feedback links that represent the dynamic interaction between the two subsystems are directly integrated into the model. This modular approach is based on state space equations, and offers two distinct advantages. First, the bridge can be modeled using standard linear, time-invariant techniques (*e.g.* a finite element model), and second, this approach permits the inclusion of significantly different levels of damping in each subsystem. With this model, changes in the modal characteristics are included by shifting the location of the pedestrian, and applying the interactive inputs directly into the bridge substructure based on the position of the pedestrian. No external disturbance is used, although a non-zero velocity is used to model the energy inserted into the system by the pedestrian. Thus, the coupled model framework described herein will support a variety of future investigations of human-induced vibrations in footbridges, and it also facilitates structural analysis conducted for design purposes. To evaluate this framework, the PBI model is created and its performance, in terms of both a pedestrian's vertical acceleration of the body center of mass (BCOM) and the structural response of the bridge, are compared with experimental data. The results demonstrate that the framework can be an efficient tool for the determination of the pedestrian biodynamic parameters, as well as the prediction of bridge response under a single pedestrian.

This paper is organized as follows. First, the mathematical substructuring approach used to represent the system dynamics is developed. The equations for each subsystem are described, and a discussion of how the inputs and outputs of each substructure interact with each other are provided. Then, an experimental study is described and the associated bridge and pedestrian models are constructed. Test subjects with different physical characteristics are considered, and a method is developed to characterize each pedestrian using data obtained while walking on a rigid floor. Finally, the predicted results of the PBI model are validated against the experimental bridge responses due to a single pedestrian, and are also compared with the results obtained using traditional models in both, time and frequency domain.

MATHEMATICAL FORMULATION

To represent the coupled subsystems, a model is developed that directly incorporates the bi-directional interactions between the bridge and pedestrian at the contact point (*i.e.* the pedestrian location). This system is partitioned into two dynamic substructures. One substructure is the footbridge, which is modeled here as a finite element (FE) model. The second substructure is the pedestrian, which is modeled as a mass-spring-damper (an oscillator). These two dynamic substructures are coupled, and each will have an influence on the other. Coupling of the two substructures is achieved by computing the response of each system at the interface, (*i.e.* the contact location at each point in time), and using it as the appropriate input for the other subsystem. This approach results in a time-varying system that considers the responses of each system as inputs to the other system (Gomez et al. 2015a). Furthermore, this framework offers flexibility through the ready use of a well-defined FE footbridge model together with a simple pedestrian biodynamic model.

In this coupled model the interaction effects, and thus the modal characteristics of the combined system, change with the position of the contact location (see Fig. 1). By decomposing the PBI system into two substructures, and feeding the inputs from the complementary dynamic system into each substructure, the dynamic interaction is directly included. The contact force generated by the pedestrian is the input to the bridge, and the structure's vertical acceleration is the input to the pedestrian model. The individual substructure equations do not vary, and to model the fully coupled system the contact location must only be modified at each time step. In the following subsections, the PBI model and the formulation of each of the substructures is discussed. Then, the interactions between the bridge and pedestrian are described such that the PBI can be represented as a feedback system. Throughout the mathematical formulation, bold, italic, and plain letters refer to matrices, vectors, and scalars, respectively.

Bridge Substructure

A typical FE model of a bridge is shown in Fig. 2. The bridge is represented as a linear, time-invariant 2-D or 3-D FE model discretized as a series of beam elements for this particular case. To demonstrate the method, only the n vertical degrees of freedom (DOFs) are considered in the analysis, while the remaining DOFs have been condensed. The number and location of each node are determined by the approximate step length of a pedestrian, and this value should be considered to be an input of the method.

The equation of motion of the general bridge substructure (BS) is represented by

$$\mathbf{M}_{\mathrm{B}}\ddot{y}\,(\mathrm{t}) + \mathbf{C}_{\mathrm{B}}\dot{y}\,(\mathrm{t}) + \mathbf{K}_{\mathrm{B}}y\,(\mathrm{t}) = L\mathrm{F}_{\mathrm{i}}^{\mathrm{con}}\,(\mathrm{t}) \tag{1}$$

where $\mathbf{M}_{\mathrm{B}}$, $\mathbf{C}_{\mathrm{B}}$, and $\mathbf{K}_{\mathrm{B}} \in \mathbb{R}^{\mathrm{n}\times\mathrm{n}}$ are the mass, damping, and stiffness matrices of the bare structure after condensation. Here, $\ddot{y}\,(\mathrm{t})$, $\dot{y}\,(\mathrm{t})$, and $y\,(\mathrm{t}) \in \mathbb{R}^{\mathrm{n}}$ are vectors containing the nodal acceleration, velocity and displacement responses, respectively. This output of the bridge subsystem will be used as the input to the pedestrian substructure. $L\,(\mathrm{t}) \in \mathbb{R}^{\mathrm{n}}$ is a column vector which varies with time and is defined by the spatial location of the pedestrian on the bridge as

$$L\,(\mathrm{t}) \;=\; \begin{bmatrix} 0 & 0 & \cdots & \underbrace{1}_{\mathrm{i^{th}}} & \cdots & \underbrace{0}_{\mathrm{n}} \end{bmatrix}^{T}. \tag{2}$$

This vector is populated with zero entries except at the DOF corresponding to nodal displacement of the deck where the pedestrian is acting. $\mathrm{F}_{\mathrm{i}}^{\mathrm{con}}\,(\mathrm{t})$ represents the force imparted by the pedestrian on the bridge at the $\mathrm{i^{th}}$ point of contact and can be written as

$$\mathrm{F}_{\mathrm{i}}^{\mathrm{con}}\,(\mathrm{t}) \;\;=\;\; \mathrm{c_p}\dot{\mathrm{w}}(\mathrm{t}) + \mathrm{k_p}\mathrm{w}\,(\mathrm{t}) \tag{3}$$

where $\dot{\mathrm{w}}(\mathrm{t})$ and $\mathrm{w}(\mathrm{t})$ are the vertical velocity and displacement of the pedestrian's body center of mass relative to the bridge, respectively. The biodynamic parameters $\mathrm{k_p}$ and $\mathrm{c_p}$ are the linear coefficients of the spring and viscous dashpot, respectively. As a result, at the $\mathrm{i^{th}}$ step, the only input applied to the bridge substructure is the distribution vector $L\,(\mathrm{t})$ times the contact force $\mathrm{F}_{\mathrm{i}}^{\mathrm{con}}\,(\mathrm{t})$. These feedback links are shown in Fig. 2.

The equation for the bridge substructure in Eq. (1) can be written in state space form. The input to this subsystem is represented by the scalar $\mathrm{F}_{\mathrm{i}}^{\mathrm{con}}$ (t) described previously. The state variables are assembled in the vector $x_b = \begin{bmatrix} y & \dot{y} \end{bmatrix}^T \in \mathbb{R}^{2\mathrm{n}\times 1}$ known as the state vector. The subsystem outputs are selected to include the displacement y, velocity $\dot{y}$, and acceleration $\ddot{y}$ responses at the nodes of the bridge, represented by the vector $z_b = \begin{bmatrix} y & \dot{y} & \ddot{y} & \ddot{\mathrm{y}}_{\mathrm{i}} \end{bmatrix}^T \in \mathbb{R}^{(3\mathrm{n}+1)\times 1}$. Note, $\ddot{\mathrm{y}}_{\mathrm{i}}(\mathrm{t})$ is the nodal acceleration at the i^{th} point, which is the point of contact. The nodal acceleration $\ddot{\mathrm{y}}_{\mathrm{i}}$ is included in the output vector to readily be used as an input to the pedestrian substructure at each time step. The resulting state space equation is:

$$\begin{bmatrix} \dot{x}_b \\ -- \\ z_b \end{bmatrix} = \begin{bmatrix} \mathbf{A}_{\mathrm{bridge}} & | & \mathbf{B}_{\mathrm{bridge}} \\ --- & -- & --- \\ \mathbf{C}_{\mathrm{bridge}} & | & \mathbf{D}_{\mathrm{bridge}} \end{bmatrix} \begin{bmatrix} x_b \\ -- \\ \mathrm{F}_{\mathrm{i}}^{\mathrm{con}} \end{bmatrix} \tag{4}$$

where

$$\mathbf{A}_{\mathrm{bridge}} = \begin{bmatrix} \mathbf{0}_{\mathrm{n}\times\mathrm{n}} & \mathbf{I}_{\mathrm{n}\times\mathrm{n}} \\ -\mathbf{M}_{\mathrm{B}}^{-1}\mathbf{K}_{\mathrm{B}} & -\mathbf{M}_{\mathrm{B}}^{-1}\mathbf{C}_{\mathrm{B}} \end{bmatrix}_{2\mathrm{n}\times 2\mathrm{n}} \qquad \mathbf{B}_{\mathrm{bridge}} = \begin{bmatrix} \mathbf{0}_{\mathrm{n}\times 1} \\ \mathbf{M}_{\mathrm{B}}^{-1} L \end{bmatrix}_{2\mathrm{n}\times 1}$$

$$\mathbf{C}_{\mathrm{bridge}} = \begin{bmatrix} \mathbf{I}_{\mathrm{n}\times\mathrm{n}} & \mathbf{0}_{\mathrm{n}\times\mathrm{n}} \\ \mathbf{0}_{\mathrm{n}\times\mathrm{n}} & \mathbf{I}_{\mathrm{n}\times\mathrm{n}} \\ -\mathbf{M}_{\mathrm{B}}^{-1}\mathbf{K}_{\mathrm{B}} & -\mathbf{M}_{\mathrm{B}}^{-1}\mathbf{C}_{\mathrm{B}} \\ -L^T\mathbf{M}_{\mathrm{B}}^{-\mathbf{1}}\mathbf{K}_{\mathrm{B}} & -L^T\mathbf{M}_{\mathrm{B}}^{-\mathbf{1}}\mathbf{C}_{\mathrm{B}} \end{bmatrix}_{(3\mathrm{n}+1)\times 2\mathrm{n}} \qquad \mathbf{D}_{\mathrm{bridge}} = \begin{bmatrix} \mathbf{0}_{2\mathrm{n}\times 1} \\ \mathbf{M}_{\mathrm{B}}^{-1} L \\ L^T\mathbf{M}_{\mathrm{B}}^{-\mathbf{1}} L \end{bmatrix}_{(3\mathrm{n}+1)\times 1} \tag{5}$$

and n, in Eq. (5), is the number of degrees of freedom of the condensed FE bridge model.

Pedestrian Substructure

Typically the pedestrian is modeled as a moving force traversing the bridge. At each step, a force profile is imparted on the bridge based on the force a pedestrian imparts on a rigid floor while walking. This method is based on measurements of ground reaction forces (GRF) using fixed force plates, which thus yield the force profile used for each step. However, this procedure does not fully account for the interactions between the pedestrian and the structure. To address this limitation, a dynamic pedestrian substructure model is used here, consisting of a SDOF oscillator with a non-zero vertical initial velocity condition as a source of excitation rather than using a ground reaction force.

In general, the energy in a human-structure coupled system is not conserved. Energy can be added by the pedestrian, or it can be dissipated by either the pedestrian or the structure. Therefore, an external energy source must be provided to simulate how a human adds energy through his/her body. A non-zero vertical initial velocity condition of the pedestrian mass is included here to incorporate the energy input that occurs during human gait described by Winter (2009) and Whittle (2014). With the human gait, two different acceleration-based sources of energy take place during the stride period. The main excitation source to this system is produced when the heel strikes the ground. A second excitation source is related to swinging of the limbs during walking (Ylli et al. 2015). By directly incorporating the first source of excitation, the vertical movement of the BCOM can be reproduced more accurately. In a subsequent section, a comparison is made between the measured vertical acceleration with the PBI predicted output in a rigid floor, showing that the model is able to add energy to the system. The pedestrian substructure (PS) is modeled here using the biodynamic characteristics as well as input parameters which have been reported in several studies (Toso et al. 2013; Pfeil et al. 2014; Ortiz-lasprilla and Caicedo 2015). The biodynamic parameters consist of a lumped mass m_p attached to a linear spring and a viscous linear dashpot with coefficients k_p and c_p, respectively. The additional input parameter is the value of the non-zero initial velocity condition $\dot{w}(t_o)$. An excitation in the PS is initiated, at each time step, by imparting a vertical initial velocity $\dot{w}(t_o)$ to the pedestrian mass at the time defined as the instant when the heel strikes the ground. This approach is capable of representing the vertical movement of the BCOM as it generates the transient effects in the bridge response due to the heel strike. The pedestrian dynamics are therefore defined by

$$m_p\ddot{w}(t) + c_p\dot{w}(t) + k_p w(t) = -m_p\ddot{y}_i(t) \tag{6}$$

where $\ddot{w}(t)$, $\dot{w}(t)$, and $w(t)$ are the vertical acceleration, velocity and displacement of the pedestrian's BCOM relative to the bridge, respectively. The input to the PS is the vertical acceleration of the bridge $\ddot{y}_i(t)$ at the contact point. The output, which was defined as the input of the complementary system in Eq. (3), is the contact force $F_i^{con}(t)$, applied to the bridge by the pedestrian, as shown in Fig. 3.

The pedestrian subsystem is also written in compact state space form. In this case, the state variables, including the relative displacement and relative velocity, are assembled in the state vector as $x_p = \begin{bmatrix} w & \dot{w} \end{bmatrix}^T \in \mathbb{R}^2$. The input is represented by $\ddot{y}_i(t)$. The outputs are represented by the vector $z_p = \begin{bmatrix} w & \dot{w} & \ddot{w} & F_i^{con} \end{bmatrix}^T \in \mathbb{R}^4$. The state space form is

$$\begin{bmatrix} \dot{x}_p \\ -- \\ z_p \end{bmatrix} = \begin{bmatrix} \mathbf{A}_{ped} & | & \mathbf{B}_{ped} \\ --- & -- & --- \\ \mathbf{C}_{ped} & | & \mathbf{D}_{ped} \end{bmatrix} \begin{bmatrix} x_p \\ -- \\ \ddot{y}_i \end{bmatrix} \tag{7}$$

where

$$\mathbf{A}_{ped} = \begin{bmatrix} 0 & 1 \\ -\frac{k_p}{m_p} & -\frac{c_p}{m_p} \end{bmatrix}_{2\times2} \quad \mathbf{B}_{ped} = \begin{bmatrix} 0 \\ -1 \end{bmatrix}_{2\times1} \quad \mathbf{C}_{ped} = \begin{bmatrix} 1 & 0 \\ 0 & 1 \\ -\frac{k_p}{m_p} & -\frac{c_p}{m_p} \\ k_p & c_p \end{bmatrix}_{4\times2} \quad \mathbf{D}_{ped} = \begin{bmatrix} 0 \\ 0 \\ -1 \\ 0 \end{bmatrix}_{4\times1} \tag{8}$$

In this study, it is assumed that the pedestrian walks at a constant velocity, which is included in the biodynamic model using the step length and pacing frequency F_p. Furthermore, the model assumes continuous contact between the pedestrian and structure, and does not distinguish between the single and double phase portions of the stance. Therefore, the possibility of separation of the pedestrian from the bridge is not considered, and the position of the pedestrian defines the contact point at each instant in time. This model could readily be extended in the future to consider a running or jumping human, or to consider variable walking speeds, as needed.

Pedestrian-bridge Interaction Model

Next, consider the interactions between the pedestrian and bridge substructures that must be included to establish the PBI feedback system. The dynamic response of the bridge is affected not only by the position of the moving mass, but also by the vertical motion of the pedestrian. Thus, during the passage of a pedestrian walking across the bridge, the pedestrian excites the bridge through the contact force at the contact point, while the bridge excites the pedestrian by its own movement at this same contact point. With this closed-loop approach, the dynamic interaction is directly integrated into the model.

The solution to these equations is obtained with a procedure that has the advantage of being simple, accurate, and explicit, yielding a global response of the coupled system. When these subsystems are solved together, this coupled and time-varying model is able to capture the interactions between the human and the structure as the position of the pedestrian on the bridge changes. In other words, the linear time-invariant pedestrian and bridge subsystems are coupled and use a time-dependent contact point, as shown in Fig. 4. Thus, this closed-loop system can be classified as a linear, time-varying dynamic system. This interactive response can be obtained for any discretized bridge and any pedestrian activity, making this pedestrian-bridge model a flexible tool.

To solve for the response of this system, the equations of motion are solved numerically for the time period $S_t = 1/F_p$ within each pedestrian step (the average step time taken by the pedestrian). Then, to simulate the response during the next step length, the final conditions of the system at the end of that step length are used as the initial conditions for the next step length. To begin, set the time to $t_k = 0$, the pedestrian first step as $i = 1$, and the initial conditions (ICs). Select a time increment Δt for the numerical integration. Typically the integration time step is chosen to correspond to a frequency that is at least 10 times the frequency of the highest mode of the bridge model. The steps for this iterative procedure are summarized in a flowchart in Fig. 5.

EXPERIMENTAL VERIFICATION

To verify the PBI model, a series of experiments were conducted to measure typical structural responses induced by a single walking pedestrian. The experimental specimen that serves as the bridge was selected based on its suitability for walking safely, its large size, and its dynamic properties. Three test subjects having different body characteristics were considered as pedestrians, and measurements were taken under various walking conditions. The objective here is to provide a realistic testbed that would exhibit significant, but representative, dynamic interactions that will be useful for assessment and verification of the model. Thus, vertical motion of the footbridge was perceptible in all tests. Comparisons are made between the measured vertical responses of this experimental specimen and the PBI model predictions. Additionally, the study considers the moving force model and moving oscillator model to assess of the capabilities and limitations of all three classes of models.

Experimental Setup and Parameter Identification

A simply-supported beam, representative of a typical girder from a full-scale bridge deck, is used as the bridge. Based on the dynamic properties of this beam, it is relatively sensitive to pedestrian-induced excitation with a pedestrian walking at a typical pace. The structure is a W_{30x132} steel beam A992 (F_y = 345 MPa and E = 200 GPa) and each end rests on a concrete block. The entire beam has a length of 15.24 m and a weight of 29.4 kN. For these experiments, the unsupported distance between the two end supports is 14.64 m (see Fig. 6). Eighteen uniaxial accelerometers are used in the experimental setup to capture the vibrations of the beam, with twelve in the vertical direction and six in the lateral (perpendicular to the long axis of the beam) direction as depicted in Fig. 7. The accelerometers are PCB Piezotronics piezoelectric sensors model 333B40 with a sensitivity of (±10%) 500 mV/g and a frequency range from 0.5 to 3 kHz.

To identify the dynamic properties of the bridge alone in this configuration, forced vibration testing is first conducted. The bridge is excited using an electrodynamic shaker placed at 1.2 m from the midspan, with the objective of capturing structural responses over a broad frequency range in both the vertical and horizontal directions. Eight forced vibration tests are conducted using either linear or logarithmic chirp signals with frequency range of 0.5-25 Hz, or a band-limited white noise (BLWN) with a bandwidth of 100 Hz, as inputs. The sampling frequency is 1024 Hz, and a low-pass filter with cut-frequency at 500 Hz is used in the data acquisition system to prevent aliasing. The duration of each test is set to 400 sec, with excitation signal amplitudes ranging from 1 to 5 V, which resulted in acceleration inputs with a PSD of 105 to 110 dB

The time history and power spectral density function (PSD) from a representative experimental acceleration response recorded during the experiments (sensor No. 8 in Fig. 7) are shown in Figs. 8(a and b). Based on the experimental data, the modal characteristics of the bridge are identified. A common curve fitting method is applied to the experimental complex frequency response function to identify the system as a ratio of polynomials in the Laplace variable s (Dyke et al. 1996). The first three vertical modes are at 2.15 Hz, 8.31 Hz and 18.12 Hz. Thus, noticeable interactions would be expected due to human-induced vibration because the first vertical natural frequency of this bridge is within the normal range of the human gait (*i.e.* 1.6-2.4 Hz) (Bachmann et al. 1995; Sétra 2006). The first two torsional modes are at 5.77 Hz and 15.25 Hz. Also, a single lateral mode is present at 10.75 Hz. These were obtained using an analyzed frequency range from 0.5 to 20 Hz. Also, the damping ratios associated with the first three vertical modes are identified to be 0.28%, 0.48% and 0.31%, respectively.

A two-dimensional FE model is developed based on the physical properties of the bridge. Torsional and lateral modes are neglected here as their effects are assumed to be insignificant for this analysis. The 2D model is then updated using the measured modal characteristics. To build the FE model, a simply-supported, homogeneous Euler-Bernoulli beam is discretized into n + 1 beam elements. The n lumped masses are located at regular distances according to the average step length of a pedestrian, and only the vertical and rotational degrees-of-freedom (DOF) are considered. Proportional damping is assumed to generate a damping matrix for the bridge substructure. The rotational DOF are condensed, yielding a bridge model with n DOF. In the condensed model the $\mathbf{M}_{\mathrm{B}}$, $\mathbf{C}_{\mathrm{B}}$, and $\mathbf{K}_{\mathrm{B}}$ matrices in Eq. (1) are thus defined, forming the bridge substructure described in Eq. (4).

Pedestrian Parameters

Three healthy subjects, one age 29 (SA), 30 (SB) and 36 (SC) respectively, with no history of postural problems, participated in a series of experiments. The applicable ethics committee approved this study, and all human subjects signed informed consent forms prior to participation. Two types of tests were conducted. In the first type of test, each subject was instructed to walk according to his/her self-selected pace. In the second type of test, a metronome was used to guide the walking pace frequency, denoted here as F_p. When the metronome was used, several pacing rates were used ranging from slow to fast (1.7, 1.8, 1.9, 2.0, 2.1, and 2.2 Hz). For each subject, the tests were first conducted on a rigid floor, and then on the flexible bridge. These tests were useful for model comparisons, as well as for parameter estimation.

The pedestrian motion was captured using a portable and non-invasive, triaxial accelerometer (STMicroelectronics k330 3-axis accelerometer). The accelerometer has a range of ±2 g and a resolution of 61 μg. The data were sampled at 100 Hz, and an elliptical low-pass filter with cut-frequency at 50 Hz was used. This device was placed close to the subject's BCOM with a belt around the waist. The device was affixed to the subject firmly above the sacrum along the spine to record trunk acceleration in the vertical direction.

To identify the parameters of the biodynamic model of the pedestrian, the experimental vertical accelerations, obtained with the pedestrian walking on a rigid floor, were used. The PBI model was used to simulate the BCOM vertical accelerations, with the bridge substructure stiffness set to a high value to minimize any dynamic interactions. Using this simulation model, the biodynamic parameters c_p and k_p as well as $\dot{w}(t_o)$ were identified through a standard constrained optimization in MATLAB® that minimizes the error between the experimental vertical BCOM acceleration and the simulated vertical acceleration of the pedestrian mass during around 20 sec. The parameter m_p is the known mass of the pedestrian. The pedestrian substructure parameters obtained for each human subject are given in Table 1. Mass ratios indicated in this table are calculated as a ratio of the mass of each subject divided by the modal mass of the first mode of the bridge alone, which is approximately 1500 kg. Note that all of these values are well within the normal range found in the literature (Archbold et al. 2011; Shahabpoor et al. 2013).

A typical time-history of the measured acceleration (solid line) and simulated acceleration (dashed line) of the human subject and the corresponding floor acceleration (dash-dotted line) are shown in Fig. 9. Here the subject SA was instructed to walk at $F_p = 1.9$ Hz using a metronome. And as an input to the model, an initial velocity, as stated previously, was used here to emulate the effect when the heel strikes the floor in each step, as shown with the dash-dotted line in Fig. 9. Clearly, the PBI model is able to capture the fundamental behavior of the vertical BCOM acceleration on a stiff surface without the use of an external force.

Experimental Verification of the PBI Model

The next step is the verification of the PBI model, in terms of its ability to capture the human-structure dynamic interactions. To do this we use the two independently identified models with the parameters established that best model the pedestrian substructure and the bridge substructure. A dynamic simulation is performed to obtain the response of the feedback system described in Eqs. (4) and (7), using a single pedestrian. The identified biodynamic parameters shown in Table 1 are used. Additionally, the moving force (MF) and moving oscillator (MO) models are considered to assess the relative capabilities and limitations of the modeling methods when interaction is present.

For all simulations, the identified model of the footbridge is used. The MO model described in (Fanning et al. 2005; Dang and Živanović 2013) uses a secondary dynamic system based on a lumped mass connected by a spring and damper with the bridge, to represent a pedestrian. For purposes of comparison, this model also utilizes the biodynamic characteristics of the pedestrian given in Table 1. Alternatively, the MF model uses a moving force determined based on the weight of the pedestrian. Both of these models also include a periodic function that has been shown to represent the vertical force applied by a walker (Bachmann et al. 1995). This function is expressed as a Fourier series multiplied by the mode shape to obtain the effective modal force, as in

$$\mathrm{F_v}\,(\mathrm{t}) = \alpha \mathrm{W} \cdot \sin\left(2\pi \mathrm{F_p t} - \varphi\right) \cdot \phi\,(\mathrm{ct}). \tag{9}$$

From Eq. (9), the single-step forcing function $\mathrm{F_v}\,(\mathrm{t})$ is represented by an amplitude corresponding to the weight of the pedestrian W, and a dynamic function, which includes the harmonic components of the pedestrian load. However, this periodic function may be limited and resolved, for practical reasons, only for the first harmonic vertical component (Sétra 2006). Thus, α and φ are the Fourier coefficient and phase lag of the first harmonic, respectively. The pace frequency is defined by $\mathrm{F_p}$, c is the constant anterior-posterior velocity of the pedestrian, $\phi(\cdot)$ is the normalized fundamental mode shape of the bridge, and t is the variable representing the time that has elapsed. The values of the first harmonic amplitude and phase lag have been chosen in this study as 0.4 and 0, respectively. Also, W, $\mathrm{F_p}$ and c are defined for each individual test based on the experimental data.

To quantitatively evaluate the models, the vertical experimental acceleration at the midspan of the footbridge is compared with the corresponding predictions from each of the models. The response is compared using an instantaneous relative error (IRE) and a normalized root mean square error (NRMSE). The difference between the simulated response $\ddot{Y}_{sim}(\mathrm{t_m})$, and the measured response $\ddot{Y}_{exp}(\mathrm{t_m})$, is computed at each time sample $\mathrm{t_m}$, and appropriately normalized and compared. The IRE is a measure of the instantaneous normalized error, and is computed at each individual time step across the N samples of the time history. The NRMSE is a measure of the overall response, and is computed using the complete response history. The IRE and NRMSE are calculated using Eqs. (10) and (11).

$$IRE(\mathrm{t_m}) = \frac{\left|\ddot{Y}^{exp}(\mathrm{t_m}) - \ddot{Y}^{sim}(t_m)\right|}{\left|\ddot{Y}^{exp}(\mathrm{t_m})\right|} \times 100\% \tag{10}$$

$$\mathrm{NRMSE} = \frac{\sqrt{\frac{1}{N}\sum_{m=1}^{N}\left[\ddot{Y}^{exp}(\mathrm{t_m}) - \ddot{Y}^{sim}(\mathrm{t_m})\right]^2}}{\max\left(\left|\ddot{Y}^{exp}(\mathrm{t_m})\right|\right)} \times 100\% \tag{11}$$

A total of 81 tests were conducted with the three subjects. 57 of these were recorded while a metronome guided the pace of the pedestrian's steps, and in the remaining 24 tests the pedestrian walked at a self-selected pace. Two representative time-histories, for two different test subjects, are shown in Figs. 10(a-d). Here the measured and simulated responses are shown, along with the corresponding value of the IRE for each individual time sample. The response of the bridge (solid line) remains zero before the pedestrian enters, gradually builds up during the pedestrian's passage, and attenuates in free vibration after the pedestrian has left the bridge. In Fig. 10(a) subject SA was instructed to walk at $F_p = 1.9$ Hz following the beat of a metronome. However, in Fig. 10(b) subject *SC* was instructed to walk at a self-selected rate and his average pace frequency was 1.98 Hz. The results for these two cases demonstrate that the PBI model (dashed line) reproduces the transient effects observed due to the heel-strike for each footfall in the same manner that the data exhibits this behavior for a walking person. To assess the performance of the PBI model, IRE values *vs.* time are shown in Figs. 10(c and d). The instantaneous relative error measure is significantly smaller with the PBI model as compared to the values obtained with the MF (dash-dotted line) and MO (dotted line) models in those representative trials.

Because this system is time-varying, a time-frequency representation using spectrograms is adopted to investigate the non-stationary characteristics of the response. The experimental and simulated response data for each model are provided (see Figs. 11(a-d)). Figs. 11(a and b) show the time-frequency analysis of the measured data only, for clarity. Obvious horizontal stripes exist in each figure around 2, 4, 6, 8 and 10 Hz due to the dominant harmonics resulting from the pace frequency associated with the pedestrian walking on the bridge. Clearly the amplitude of the structural response increases significantly in the frequency range between 1.7 and 2.3 Hz because this dominant first harmonic is close to the first vertical natural frequency of the bridge ($F_1 = 2.15$ Hz).

We also examine the frequency variations that occur with the various models (MF, MO and PBI models), as compared to the frequency variations present in the measured responses. Figs. 11(c and d) show a zoomed-in plot over a limited frequency range extracted from the spectrogram in Figs. 11(a and b). Here one can observe the variations in the power spectral density when a pedestrian crosses the bridge. In Figs. 11(c and d), the horizontal dotted line represents the fundamental frequency of the bridge alone, where it is not affected by the presence of the pedestrian. The solid line indicates the frequency associated with the maximum value of the power spectral density at each point in time. In both cases, when the subject walks at a specified pace of 1.9 Hz (see Fig. 11(c)) or at a self-selected rate with an estimated average pace frequency of 1.98 Hz (see Fig. 11(d)), there is a significant variation in the frequency content of the experimental response with time. This variation can be attributed to a combination of: (1) the mass distribution due to the pedestrian's location; and (2) the forced response in the pedestrian-bridge system due to the quasi-periodic loading at pace frequency F_p and its harmonics. Additionally, the corresponding lines that are provided for the MF and MO models indicate that in this case these models do not account for the significant dynamic interaction effects. The variations in the accuracy of the predicted responses of the coupled-system are more pronounced when the pace frequency is closer to the vertical natural frequency of the structure. Better agreement is observed with the PBI model in those representative trials.

The NRMSE obtained with each model was used to obtain a single value for each of the 57 metronome-based experimental trials, and these results are summarized in Figs. 12(a-c). Because several repetitions were performed for each of the tests, the mean value and standard deviation of the NRMSE values are computed for each test configuration. These values are shown for each of the corresponding pace frequencies considered, where the pace frequencies are normalized against the first vertical natural frequency of the structure. The NRMSE values associated with the responses of the MF and MO models are typically larger than those of the PBI model. Moreover, the MF and MO models produce particularly large NRMSE values when the frequency ratio F_p/F_1 are in the range between 0.7 to 0.9. Here, the dynamic interaction is low and the behavior is dominated by the forced response of the structure. Furthermore, both the MF and MO models overestimate the system response when the F_p/F_1 is close to the first vertical natural frequency of the bridge (*i.e.* 0.9 to 1.05). This result means that MF and MO have limited capacity to take into account the interaction between the two subsystems. However, the PBI model exhibits significantly smaller normalized errors because the model accounts for the influence of the bridge on pedestrian on the dynamics.

The responses are examined from an alternate perspective in Figs. 13(a-c). These figures show the range of variation of the peak estimated acceleration of the responses versus the normalized pace frequency. The upper and lower bounds provided are defined by the mean and standard deviation of the maximum absolute values of the response. Both the experimental and PBI prediction results are given for each frequency ratio of interest in the tests using the metronome. Here the mean of the peak values of the simulated responses have nearly the same amplitude as the peaks of the measured responses. And as expected, more dynamic interaction occurs between the two subsystems when the frequency ratio is close to one. Additionally, 24 experiments were conducted at a self-selected pace frequency. These responses were analyzed and the corresponding peak responses are represented with diamonds in Figs. 13(a-c). It can be concluded that the PBI model yields an accurate prediction of the peak acceleration of the pedestrian-bridge system as indicated by the discrete circles, even when the pedestrian walks naturally. Indeed for SB, a pedestrian that walked at a slower speed than in the metronome, the responses are typically in agreement with the experimental data. Clearly the PBI model is able to capture the dominant coupled dynamics of the pedestrian-bridge system.

CONCLUSIONS

A pedestrian-bridge interaction model has been presented herein for predicting the dynamic response of a footbridge traversed by a single pedestrian. The strongly coupled scheme considers the pedestrian and bridge as an integrated system. The formulation facilitates modeling of this complex dynamic interaction problem using separate models of the two substructures, while coupling their dynamics through a moving contact point in a closed-loop arrangement. This framework uses simple dynamic expressions for the bridge and pedestrian subsystems which can readily be reproduced for analysis or even design purposes. Furthermore, the flexibility of this framework could easily incorporate more complex models of either pedestrians or bridges, and could also be used as a framework to consider advanced damping devices or structural control systems.

Embedded in the model is a non-zero initial velocity condition, representing the energy inserted into the system at each step by the human. This approach is inspired by the transient response observed in the experimental accelerations, and in simulation is shown to produce quite similar responses. The initial velocity produces a vertical BCOM movement, similar to the way that human trunk moves, and this model is validated with measurement of the trunk motion on a rigid floor. Also, a method is established and verified here to identify reliable biodynamic properties (*i.e.* stiffness and damping) for a simple model of the human body.

The predicted acceleration responses with the PBI, the moving force (MF), and the moving oscillator (MO) models were compared with experimental acceleration data. Different gait speeds were considered while a single human subject traversed a previously identified steel beam that served as a bridge. Three different human subjects participated. The PBI model was found to be better at predicting the variations in the natural frequency of the coupled system, as well as the peak responses of the coupled system. The PBI model is found to be effective for predicting the bridge response when dynamic interactions are present.

ACKNOWLEDGMENTS

This work was financially supported by the Colombia-Purdue Institute for Advanced Scientific Research (CPI), the Universidad del Valle and Purdue University. The authors also would like to acknowledge Professor Robert Connor from Purdue University for providing the steel beam used in this study. The authors also would like to thank Sandra Villamizar and Christian Silva for their help with the data collection.

REFERENCES

Alexander, R. (1995). "Simple models of human movement." *Applied Mechanics Reviews*, 48(8), 461.

Archbold, P., Keogh, J., Caprani, C., and Fanning, P. (2011). "A parametric study of pedestrian vertical force models for dynamic analysis of footbridges." *EVACES – Experimental Vibration Analysis for Civil Engineering Structures*, Varenna, Italy, 35–44.

Bachmann, H., Ammann, W. J., Deischl, F., Eisenmann, J., Floegl, I., Hirsch, G. H., Klein, G. K., Lande, G. J., Mahrenholtz, O., Natke, H. G., et al. (1995). *Vibration problems in structures: practical guidelines*. Birkhäuser.

Blanchard, J., Davies, B. L., and Smith, J. W. (1977). "Design criteria and analysis for dynamic loading of footbridges." *Proceeding of a Symposium on Dynamic Behaviour of Bridges at the Transport and Road Research Laboratory*, Crowthorne, UK, 90–106.

Bocian, M., Macdonald, J. H. G., and Burn, J. F. (2013). "Biomechanically inspired modeling of pedestrian-induced vertical self-excited forces." *Journal of Bridge Engineering*, 18(12), 1336–1346.

Dallard, P., Fitzpatrick, T., Flint, A., Low, A., Smith, R., Willford, M., and Roche, M. (2001). "London Millenium bridge: pedestrian-induced lateral vibration." *Journal of Bridge Engineering*, 6(6), 412–417.

Dang, H. V. and Živanović, S. (2013). "Modelling pedestrian interaction with perceptibly vibrating footbridges." *FME Transactions*, 41(4), 271–278.

Dyke, B. S. J., Member, S., Member, B. F. S. J., Quast, P., Sain, M. K., Jr, D. C. K., and Soong, T. T. (1996). "Acceleration feedback control of mdof structures." 122(9), 907–918.

Eckhardt, B., Ott, E., Strogatz, S. H., Abrams, D. M., and McRobie, A. (2007). "Modeling walker synchronization on the Millennium bridge." *Physical Review E - Statistical, Nonlinear, and Soft Matter Physics*, 75(2), 1–10.

Ellingwood, B. and Tallin, A. (1984). "Structural serviceability: floor vibrations." *Journal of Structural Engineering*, 110(2), 401–418.

Fanning, P., Archbold, P., and Pavic, A. (2005). "A novel interactive pedestrian load model for flexible footbridges." *Proceeding of the 2005 Society for Experimental Mechanics Annual Conference on Experimental and Applied Mechanics*, Portland, OR, 7–9.

Gomez, D., Dyke, S. J., and Maghareh, A. (2015a). "Enabling role of hybrid simulation across NEES in advancing earthquake engineering." *Smart Structures and Systems*, 15(3), 913–929.

Gomez, D., Silva, C., Dyke, S., and Thomson, P. (2015b). "Interactive platform to include human-structure interaction effects in the analysis of footbridges." *Proceedings of the XXXIII Conference and Exposition on Structural Dynamics (IMAC 2015)*, Orlando, FL, 1110–1117.

Jimenez-Alonso, J. F., Saez, A., Caetano, E., and Magalhaes, F. (2016). "Vertical crowd – structure interaction model to analyze the change of the modal properties of a footbridge." *Journal of Bridge Engineering*, 21(8), 1–19.

Kim, S. H., Cho, K. I., Choi, M. S., and Lim, J. Y. (2008). "Development of human body model for the dynamic analysis of footbridges under pedestrian induced excitation." *International Journal* *of Steel Structures*, 8(4), 333–345.

Macdonald, J. (2009). "Lateral excitation of bridges by balancing pedestrians." *Proceedings of the Royal Society A: Mathematical, Physical and Engineering Sciences*, 465(2104), 1055–1073.

Mochon, S. and McMahon, T. (1980). "Ballistic walking: an improved model." *Mathematical Biosciences*, 52, 241–260.

Onyshko, S. and Winter, D. (1980). "A mathematical model for the dynamics of human locomotion." *Journal of Biomechanics*, 13(4), 361–368.

Ortiz-lasprilla, A. R. and Caicedo, J. M. (2015). "Comparing closed loop control models and mass-spring-damper models for human structure interaction problems." *Proceedings of the XXXIII Conference and Exposition on Structural Dynamics (IMAC 2015)*, Orlando, FL, 67–74.

Pfeil, M., Amador, N., Pimentel, R., and Vasconcelos, R. (2014). "Analytic – numerical model for walking person – footbridge structure interaction." *Proceedings of the 9th International Conference on Structural Dynamics, EURODYN 2014*, Porto, Portugal, 1079–1086.

Qin, J. W., Law, S. S., Yang, Q. S., and Yang, N. (2013a). "Finite element analysis of pedestrian-bridge dynamic interaction." *Journal of Applied Mechanics*, 81(4), 1–15.

Qin, J. W., Law, S. S., Yang, Q. S., and Yang, N. (2013b). "Pedestrian-bridge dynamic interaction, including human participation." *Journal of Sound and Vibration*, 332(4), 1107–1124.

Rainer, J. H., Pernica, G., and Allen, D. E. (1988). "Dynamic loading and response of footbridges." *Canadian Journal of Civil Engineering*, 15, 66–71.

Ricciardelli, F. and Pizzimenti, A. D. (2007). "Lateral walking-induced forces on footbridges." *Journal of Bridge Engineering*, 12(6), 677–688.

Roberts, T. M. (2003). "Synchronised pedestrian excitation of footbridges." *Proceedings of ICE, Bridge Engineering*, 156(4), 155–160.

Roos, I. (2009). "Human induced vibration on footbridges: Application and comparison of pedestrian load models." M.S. thesis, Delft University of Technology, Netherlands.

Sachse, R., Pavic, A., and Reynolds, P. (2003). "Human-structure dynamic interaction in civil engineering dynamics: A literature review." *Shock and Vibration Digest*, 35(1), 3–18.

Sánchez, J., Gomez, D., and Thomson, P. (2013). "Analysis of human-structure interaction in footbridges in Santiago de Cali." *Dyna*, 80(177), 86–94.

Sétra (2006). "Footbridges, assessment of vibrational behaviour of footbridges under pedestrian loading." *Technical guide, Service d'Etudes Techniques des Routes et Autoroutes*, Paris, France.

Shahabpoor, E., Pavic, A., and Racic, V. (2013). "Using MSD model to simulate human-structure interaction during walking." *Topics in Dynamics of Civil Structures, Volume 4: Proceedings of the 31st IMAC, A Conference on Structural Dynamics, 2013*, Vol. 4, 357–364.

Toso, M. A., Gomes, H. M., Silva, F. T., and Pimentel, R. L. (2013). "A biodynamic model fit for vibration serviceability in footbridges using experimental measurements in a designed force platform for vertical load gait analysis." *Icem15: 15Th International Conference on Experimental Mechanics*, Vol. 22, Porto, Portugal, 23–33.

Van Nimmen, K., Lombaert, G., De Roeck, G., and Van den Broeck, P. (2014). "Vibration serviceability of footbridges: Evaluation of the current codes of practice." *Engineering Structures*, 59, 448–461.

Venuti, F., Bruno, L., and Bellomo, N. (2007). "Crowd dynamics on a moving platform: Mathematical modelling and application to lively footbridges." *Mathematical and Computer Modelling*, 45(3-4), 252–269.

Whittington, B. R. and Thelen, D. G. (2009). "A Simple mass-spring model with roller feet can induce the ground reactions observed in human walking." *Journal of Biomechanical Engineering*, 131(1), 011013.

Whittle, M. W. (2014). *Gait analysis: an introduction*. Butterworth-Heinemann.

Winter, D. A. (2009). *Biomechanics and motor control of human movement*. John Wiley & Sons.

Ylli, K., Hoffmann, D., Willmann, A., Becker, P., Folkmer, B., and Manoli, Y. (2015). "Energy harvesting from human motion: Exploiting swing and shock excitations." *Smart Materials and Structures*, 24(2), 25029.

Živanović, S., Diaz, I. M., and Pavić, A. (2009). "Influence of walking and standing crowds on structural dynamic properties." *Proceedings of the the 27th IMAC Conference*, Orlando, Florida

USA.

Živanović, S., Pavić, A., and Ingólfsson, E. (2010). "Modelling spatially unrestricted pedestrian traffic on footbridges." *Journal of Structural Engineering*, 136(10), 1296–1308.

Živanović, S., Pavić, A., and Reynolds, P. (2005). "Vibration serviceability of footbridges under human-induced excitation: A literature review." *Journal of Sound and Vibration*, 279(1-2), 1–74.

Zuo, D., Hua, J., and Van Landuyt, D. (2012). "A model of pedestrian-induced bridge vibration based on full-scale measurement." *Engineering Structures*, 45, 117–126.

List of Tables

TABLE 1. Bio-dynamic Parameters Obtained on a Rigid Floor

Subject	$\mathbf{m_p}$ $[kg]$	$\mathbf{c_p}$ $[kg\ s^{-1}]$	$\mathbf{k_p}$ $[N\ m^{-1}]$	$\dot{\mathbf{w}}(\mathbf{t_o})$ $[m\ s^{-1}]$	**Mass ratio** [%]
SA	56	212.5	14000	0.30	3.73
SB	97	501.4	20000	0.38	6.47
SC	72	273.2	18000	0.22	4.80

List of Figures

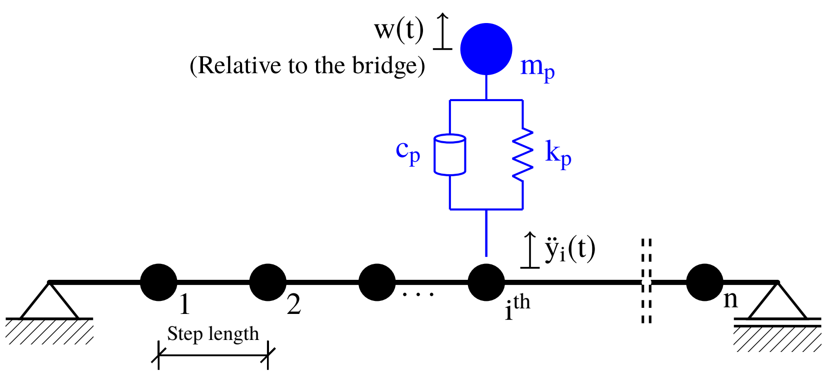

Fig. 1. Model of the pedestrian-bridge coupled system

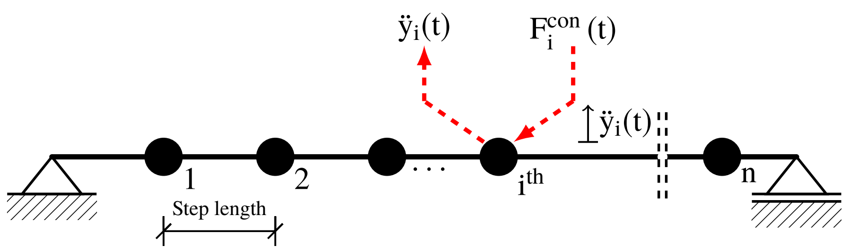

Fig. 2. Discretized bridge substructure

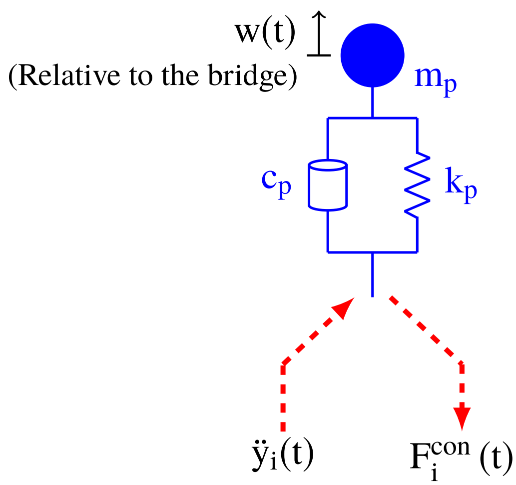

Fig. 3. Pedestrian substructure

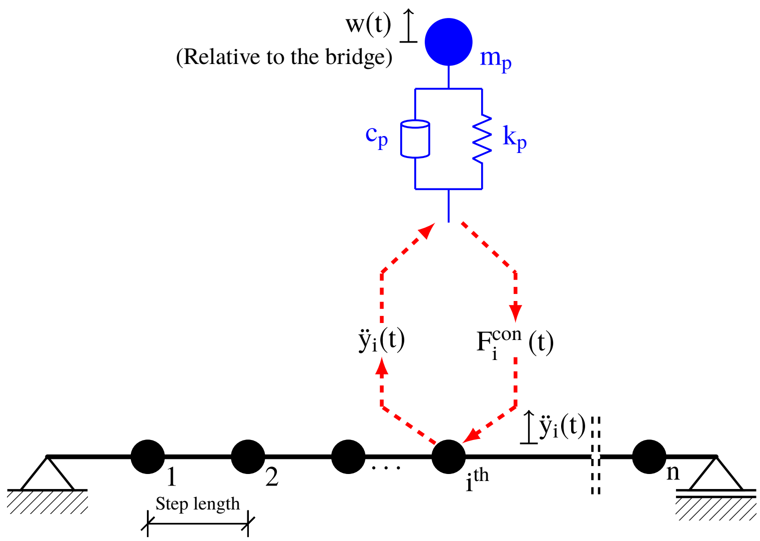

Fig. 4. Pedestrian-bridge feedback model

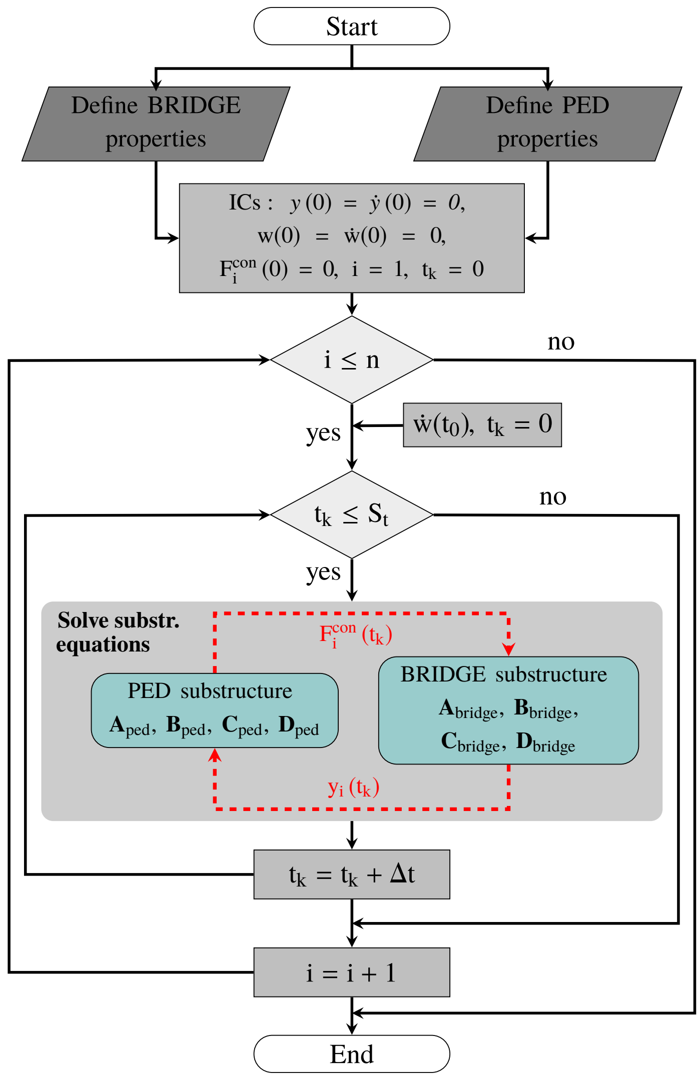

Fig. 5. Flowchart of the solution procedure

Fig. 6. Experimental setup of full-scale steel beam

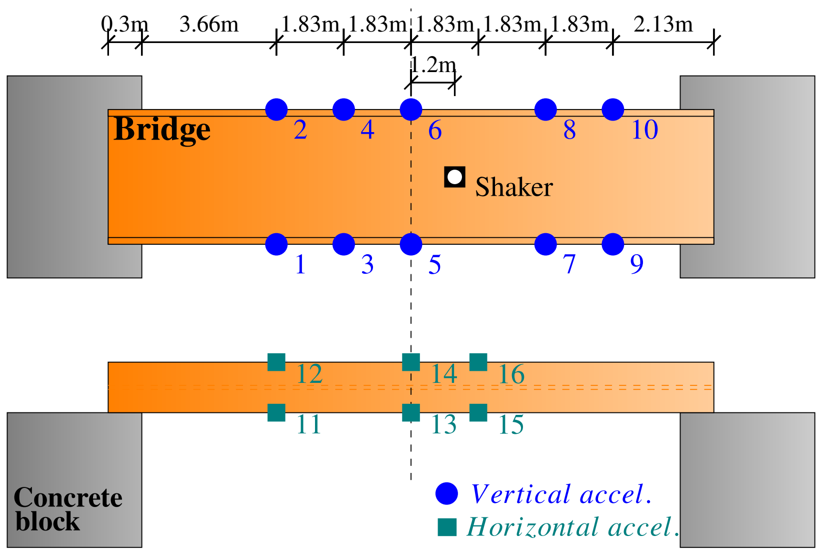

Fig. 7. Location of 18 accelerometers, with 12 in the vertical and 6 in the horizontal direction

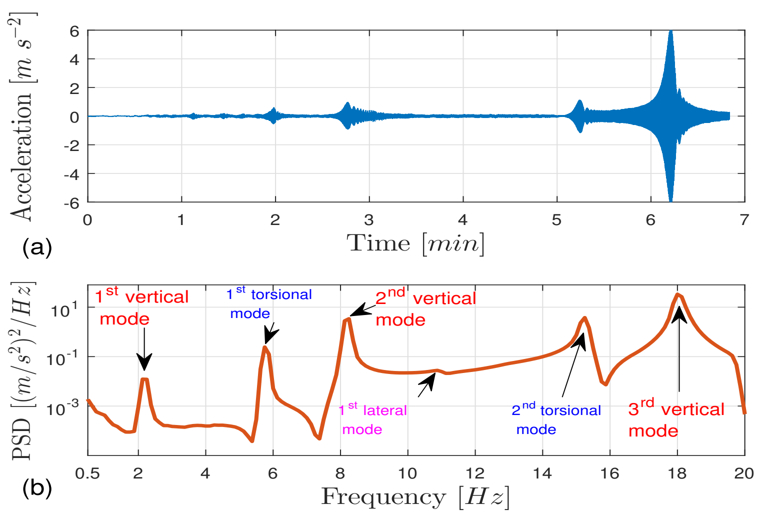

Fig. 8. Bridge substructure acceleration measured response: (a) time history; (b) PSD

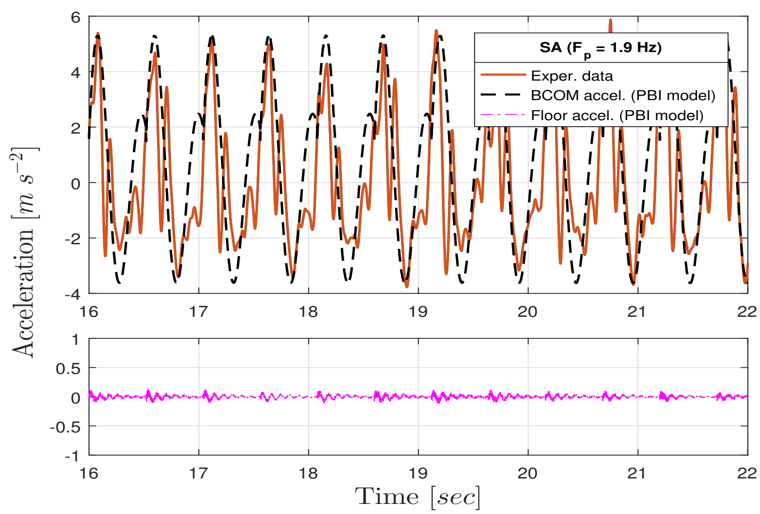

Fig. 9. BCOM acceleration in a rigid floor (subject SA)

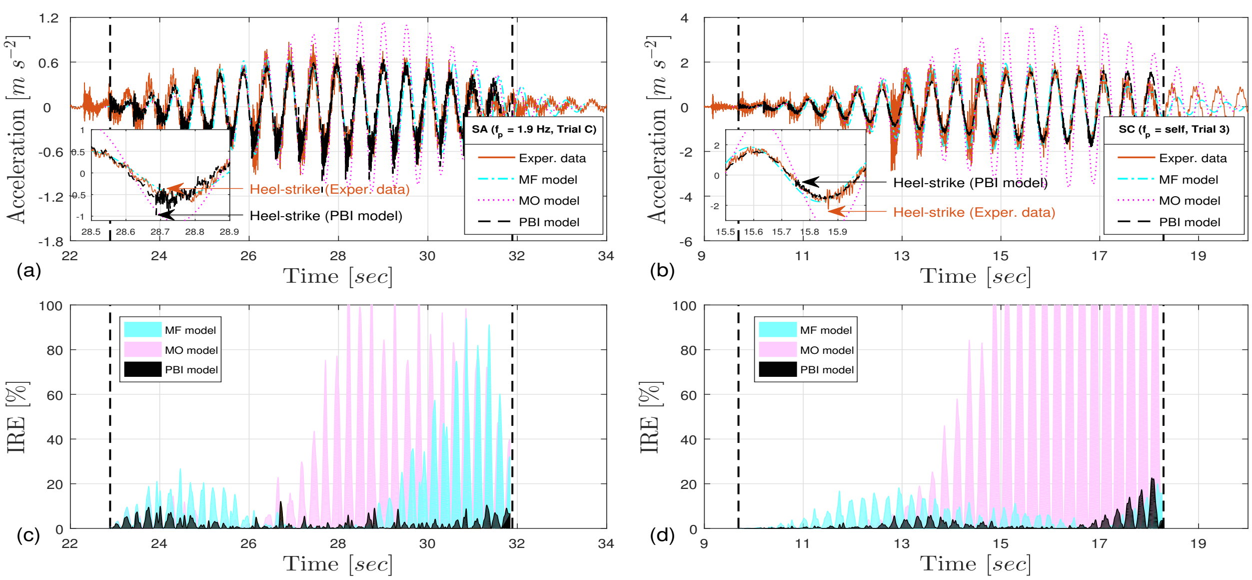

Fig. 10. Measured and predicted vertical acceleration responses at midspan of the bridge for a single pedestrian: (a) using the metronome at F_p = 1.9 Hz; (b); self-selected pace frequency; (c and d) IRE comparison. [Dashed vertical lines indicate the times at which the pedestrian enters and leaves the bridge]

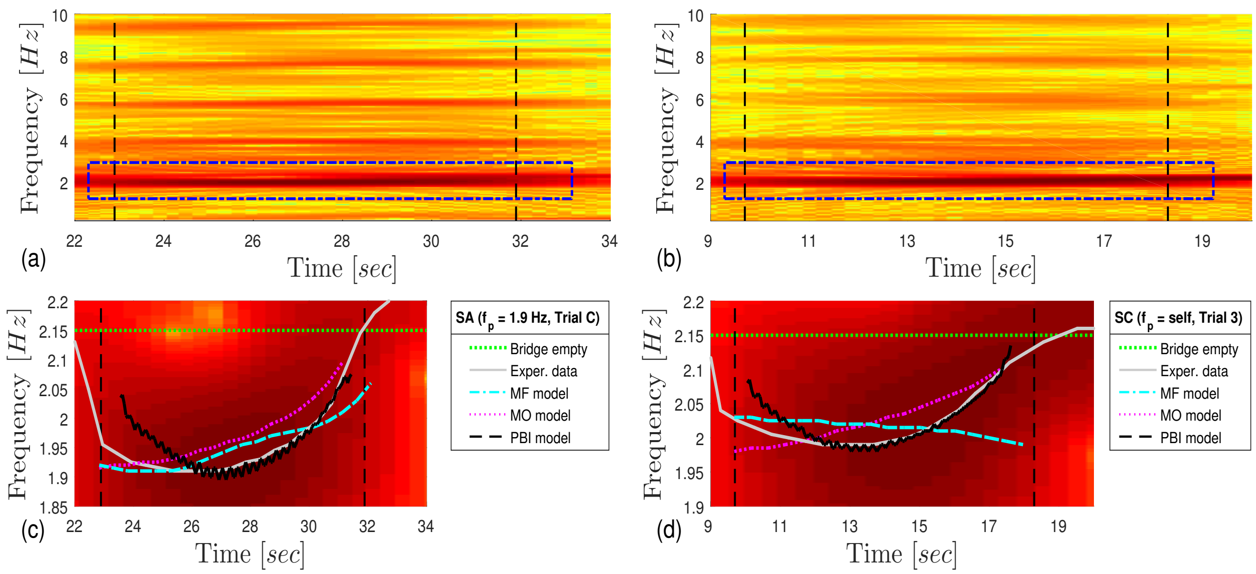

Fig. 11. Time-frequency representation to single pedestrian: (a and b) measured responses of bridge midspan; (c and d) zoom-in plot of a frequency range from the spectrogram including measured and predicted vertical acceleration variation responses. [Dashed vertical lines indicate the times at which the pedestrian enters and leaves the bridge]

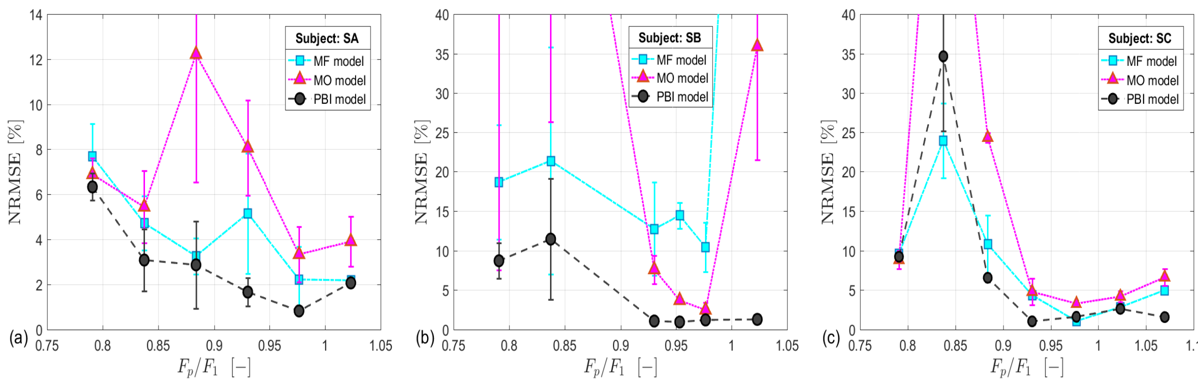

Fig. 12. Mean and standard deviation values of the NRMSE for test subjects: (a) *SA*; (b) *SB*; (c) *SC*

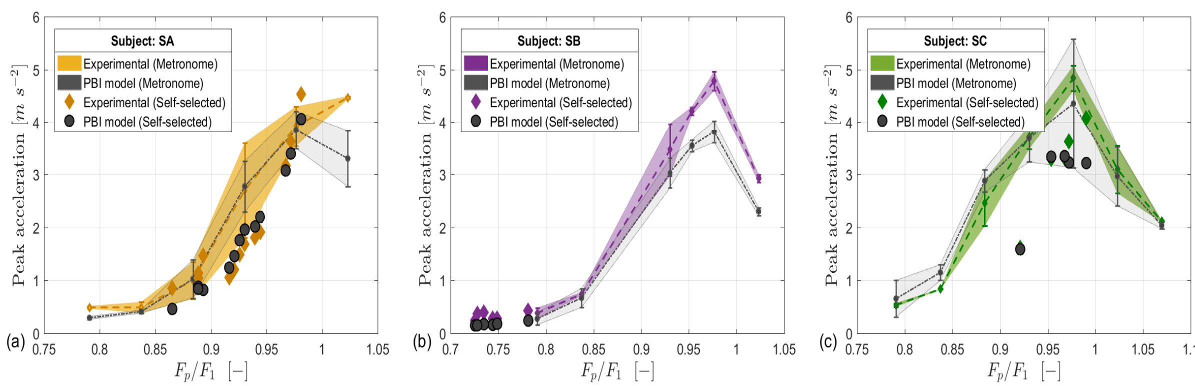

Fig. 13. Peak acceleration for test subjects: (a) *SA*; (b) *SB*; (c) *SC*